

Land–Atmosphere Interactions during a Northwestern Argentina Low Event

CELESTE SAULO

Departamento de Ciencias de la Atmósfera y los Océanos, Universidad de Buenos Aires, and Centro de Investigaciones del Mar y la Atmósfera (CONICET-UBA), Buenos Aires, Argentina

LORENA FERREIRA

Departamento de Ciencias de la Atmósfera y los Océanos, Universidad de Buenos Aires, and Servicio Meteorológico Nacional, Buenos Aires, Argentina

JULIA NOGUÉS-PAEGLE

Department of Meteorology, University of Utah, Salt Lake City, Utah

MARCELO SELUCHI

Centro de Previsao de Tempo e Estudos Climaticos (CPTEC)-INPE, Cachoeira Paulista, Brazil

JUAN RUIZ

Departamento de Ciencias de la Atmósfera y los Océanos, Universidad de Buenos Aires, and Centro de Investigaciones del Mar y la Atmósfera (CONICET-UBA), Buenos Aires, Argentina

(Manuscript received 16 September 2009, in final form 7 January 2010)

ABSTRACT

The impact of changes in soil moisture in subtropical Argentina in rainfall distribution and low-level circulation is studied with a state-of-the-art regional model in a downscaling mode, with different scenarios of soil moisture for a 10-day period. The selected case (starting 29 January 2003) was characterized by a northwestern Argentina low event associated with well-defined low-level northerly flow that extended east of the Andes over subtropical latitudes. Four tests were conducted at 40-km horizontal resolution with 31 sigma levels, decreasing and increasing the soil moisture initial condition by 50% over the entire domain, and imposing a 50% reduction over northwest Argentina and 50% increase over southeast South America. A control run with NCEP/Global Data Assimilation System (GDAS) initial conditions was used to assess the impact of the different soil moisture configurations.

It was found that land surface interactions are stronger when soil moisture is decreased, with a coherent reduction of precipitation over southern South America. Enhanced northerly winds result from an increase in the zonal gradient of pressure at low levels. In contrast, when soil moisture is increased, smaller circulation changes are found, although there appears to be a local feedback effect between the land and precipitation. The combined effects of changes in the circulation and in local stratification induced by soil wetness modifications, through variations in evaporation and Convective Available Potential Energy (CAPE), are in agreement with what has been found by other studies, resulting in coherent modifications of precipitation when variations of CAPE and moisture flux convergence mutually reinforce.

1. Introduction

The crucial role of land–atmosphere feedbacks on climate has long been recognized in the climate modeling

community. Nevertheless, large uncertainties in the representation of surface processes continue to lead to poor understanding of land–atmosphere interactions. More recent, significant improvements of land surface process modeling have been made. These improvements are related to development of more sophisticated land surface models that, combined with available observations of soil characteristics, provide an increasingly reliable

Corresponding author address: Celeste Saulo, Ciudad Universitaria, 2do piso, pabellon II, 1428, Buenos Aires, Argentina.
E-mail: saulo@cima.fcen.uba.ar

global picture of soil variables, including one generated by the Global Land Data Assimilation System (Rodell et al. 2004).

Among soil variables, much interest focuses on soil moisture, given its influence on precipitation and its variability, particularly the positive feedback through which anomalous precipitation conditions are self-sustained and amplified by the land surface state. Dirmeyer et al. (2009), using land memory estimations, provide a framework to recognize the areas where this kind of feedback is more evident. They show that, during summer, a significant portion of South America is characterized by soil moisture memory below 15 days. According to this result, precise initialization of land surface conditions would have a positive impact in short- to medium-range predictability but might not be significant at seasonal time scales.

There are very few studies addressing the issue of land–atmosphere coupling over South America, and most of these analyze impact of surface conditions on precipitation at monthly or seasonal time scales (Sörensson et al. 2010; Collini et al. 2008; Grimm et al. 2007; Xue et al. 2006, among others). These studies suggest that soil moisture has an important role on precipitation variability and in the monsoon development. However, if soil memory is indeed bounded by a 15-day period—as shown by Dirmeyer et al. (2009)—monthly means may provide weak representations of land–atmosphere coupling over large areas in South America and actual feedbacks may be hidden. Consequently, inferences obtained from climate studies could be complemented by individual case examinations. This hypothesis constitutes our rationale to select a particular case study in order *to analyze in more detail the pathways for land–atmosphere coupling over our region of concern, which covers southern and southeastern South America*. In this context, it is of interest to understand which mechanisms account for precipitation variability occurring as a consequence of changes in soil conditions: are they mostly related to local moisture recycling and/or to changes in circulation? Answering these questions will provide useful hints to focus on the specific improvements needed to achieve the theoretical limit of predictability, at least to the extent it can be realized by current state-of-the-art models. Moreover, the approach permits relatively detailed analyses of thermal and dynamical responses for time scales in which forecast models retain deterministic predictability skill and also incorporates a state-of-the-art model and special field observations. Similar methodology has been followed by Trier et al. (2008), Gallus and Segal (1999), and Zhong et al. (1996), among many others, when analyzing physical processes involved in land–atmosphere interactions under specific weather types (i.e., organized convection, cold fronts, low-level jets, etc.).

Selection of a particular event is not a trivial problem, since, ideally, the prevailing synoptic circulation should remain quasi-stationary and should allow for the manifestation of coherent land–atmosphere interactions. On the other hand, under this kind of approach, model performance is not a minor issue, since day-by-day evolution of the system has to be correctly simulated. With these requirements in mind, we selected a northwestern Argentina low (NAL) event, characterized by an enhanced low-level jet (LLJ), rather persistent synoptic circulation, and high frequency of occurrence during summertime (Ferreira 2008). Previous studies (Seluchi et al. 2003; Saulo et al. 2004a, among others) support the assumption that this kind of event is particularly sensitive to surface heating as well as enhanced soil moisture/surface temperature gradient, and are associated with heavy rainfall that is mostly concentrated over southeastern South America (SESA), at the exit region of the LLJ. So it is likely that this system is suitable to develop an understanding of the physical mechanisms involved in the soil moisture–rainfall feedback. Moreover, given that the selected situation is in close correspondence with the first principal component identified by Compagnucci and Salles (1997) in summer, enhanced understanding should aid in the description of a significant portion of the processes underlying land–atmosphere coupling during the warm season.

To show how soil moisture–precipitation–circulation interaction takes place, and to see the impact of soil wetness changes on this interaction, we designed a series of sensitivity studies that are described in section 2. Besides addressing the aforementioned issues we also expect them to serve as first indications on how land-use changes related with human activities affect weather. Following a detailed analysis of the case study and the experimental design (section 2), sections 3 and 4 are devoted to the examination of impacts on precipitation and circulation, respectively, while the main conclusions are summarized in section 5.

2. Case study and model design

Several circulation patterns can be clearly identified during the warm season in the vicinity of South America, including the well-documented intraseasonal seesaw pattern (Nogués-Paegle and Mo 1997). This pattern explains precipitation enhancement over the South Atlantic convergence zone (SACZ) in one phase and over SESA in the opposite phase. The South America low-level jet (SALLJ; Marengo et al. 2004; Vera et al. 2006a, and references therein) tends to be more active in the latter phase and is associated with a thermal-orographic low pressure system, centered around 28°S, immediately east of the Andes. This system, locally known as the

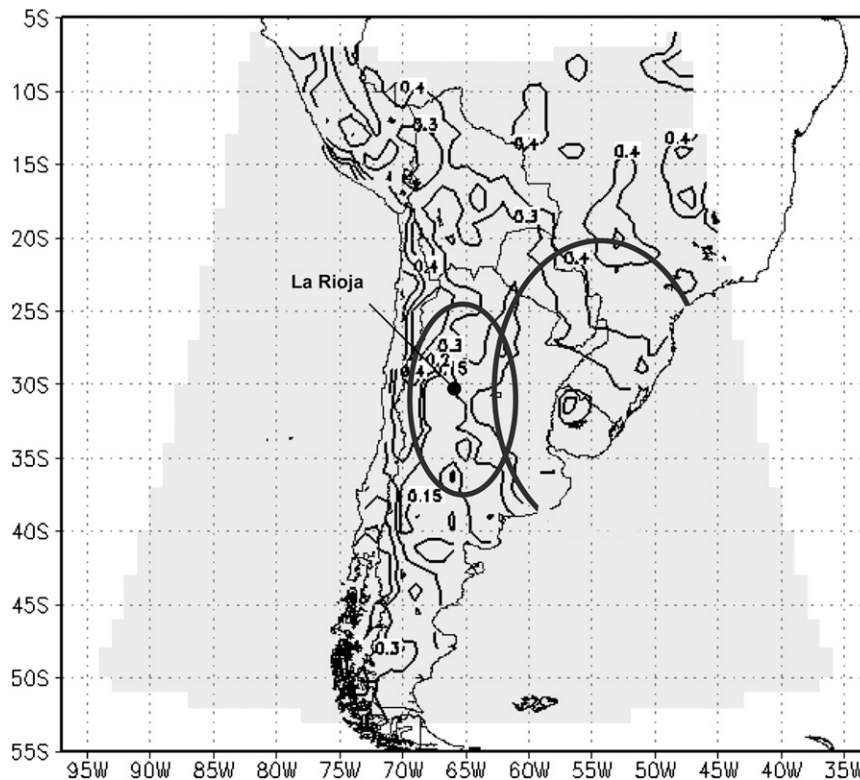


FIG. 1. Model domain (shaded) and soil wetness initial condition (contours, $\text{m}^3 \text{m}^{-3}$) for the control run at 1200 UTC 29 Jan 2003. Ellipses indicate areas where soil wetness was modified in E2 and E4 (left and right ellipses, respectively). The position of La Rioja station is also indicated.

NAL, helps to increase the meridional penetration of the SALLJ in such a way that precipitation at the exit region of the jet occurs over SESA (Salio et al. 2002; Saulo et al. 2004a). Only a few papers have focused upon the NAL. This system was initially identified by Schwerdtfeger (1950) and then studied by Lichtenstein (1980), who introduced the idea of “thermal orographic” system to synthesize the main processes operating on the NAL. More recently, Seluchi et al. (2003) discussed the mechanisms associated with the NAL life cycle in two case studies, and Ferreira (2008) extended this analysis with a climatology of the NAL. One interesting aspect of this low pressure system is that it is very sensitive to the surface energy budget and also responds to orographic effects resulting from the interaction of the Andes with the progression of midlatitude baroclinic systems approaching South America. Seluchi et al. (2003) document large surface warming at NAL locations, which results from a succession of days with clear skies over an area characterized by very dry soils with shrub-type vegetation. The obvious dependence of surface warming on land surface characteristics suggests that changes in surface conditions may significantly modify NAL strength

and SALLJ intensity, through geostrophic response (Saulo et al. 2004a).

These results in combination with process studies over North America (Fast and McCorcle 1990; Zhong et al. 1996; Paegle et al. 1996; Wu and Raman 1997), which show that the Great Plains low-level jet exhibits strong sensitivity to changes in soil moisture and land surface contrasts, provide partial motivation to analyze how changes in surface conditions may alter the LLJ and the associated precipitation over South America. With this objective in mind, we selected a NAL event, since it combines sensitivity to surface conditions with a well-developed low-level jet.

The selected NAL event occurred between 29 January and 7 February 2003 and has been previously documented by Saulo et al. (2004b), using an enhanced upper-air network and special data obtained during a National Oceanic and Atmospheric Administration (NOAA) P3 flight, available through the South America Low-Level Jet Field Experiment (SALLJEX; Vera et al. 2006b). The Weather Research and Forecasting model (WRF) version 2.0 (Skamarock et al. 2005) is used to perform all experiments in a domain centered over the area affected

TABLE 1. Model experiments.

Soil wetness initial condition	
E1	50% reduction over the entire domain
E2	50% reduction over northwest Argentina
E3	50% increase over the entire domain
E4	50% increase over SESA
CTRL	NCEP/GDAS analysis

by the NAL and the SALLJ shown in Fig. 1. Many experiments were carried out to define model settings in order to ensure a reasonable representation of this long lasting event. The model domain was adjusted so that the domain provided a satisfactory representation of the system. The model was run in nonhydrostatic mode with 40-km grid spacing in the horizontal and 31 vertical levels. We utilize the Eta grid-scale cloud and precipitation microphysics scheme (Ferrier et al. 2002); convection was parameterized using the Kain–Fritsch method (Kain 2004); and the Rapid Radiative Transfer Model (Mlawer et al. 1997) and Dudhia (1989) scheme are used to represent radiative fluxes in long and short waves, respectively. The Yonsei University (YSU; Hong and Pan 1996) scheme was selected for parameterizing boundary layer processes and the Noah land surface model to represent surface processes (Chen and Dudhia 2000). All simulations were initialized at 1200 UTC 29 January 2003 and run for 10 days. Initial and boundary conditions with 6-h intervals are derived from the National Centers for Environmental Prediction (NCEP) Global Data Assimilation System (GDAS) analysis. Land-use categories employed by the WRF are those generated by the U.S. Geological Survey (USGS) land-use/land-cover system (Anderson et al. 1976). All experiments are listed in Table 1; the only difference between them is their initial condition

of soil wetness, the variable that represents moisture content in a soil column. The run initialized with GDAS soil wetness will be referred to as the control run (CTRL).

The experiment design is conceived to address the following questions: Is SESA precipitation modified by changes in soil wetness at regional scales? What kind of feedbacks, due to these changes, can be identified in the circulation at synoptic time scales? Experiments E1 and E3 should help to answer these issues, since they correspond to 50% decrease–increase, respectively, of soil wetness over the model domain. Although these experiments are unrealistic in the sense that there are no foreseeable reasons to expect such changes to occur over such a large area, they are useful to identify possible linkages between soil states and the circulation. It should be stressed that soil moisture changes proposed here are similar to those applied in many sensitivity studies (e.g., Zhong et al. 1996; Paegle et al. 1996; Gallus and Segal 1999; Collini et al. 2008; among others).

We also wish to evaluate the impact of enhanced soil moisture gradients (drier to the west or moister to the east) on the LLJ and related precipitation. This goal motivates experiments E2 and E4, which are similar to E1 and E3 but with moisture changes bounded by two specific areas: drier conditions (E2) are limited to northwestern Argentina area while moister ones (E4) affect SESA (see Fig. 1 to locate the subareas subject to these soil wetness changes). In particular, this last experiment could be considered representative of an increase in agricultural activity and associated irrigation over one of the regions with greater economic activity in South America. In this sense we cover, at least partially, an analysis of effects linked with human activities in a more realistic way.

To validate model performance we select specific variables whose representation is critical for the processes of

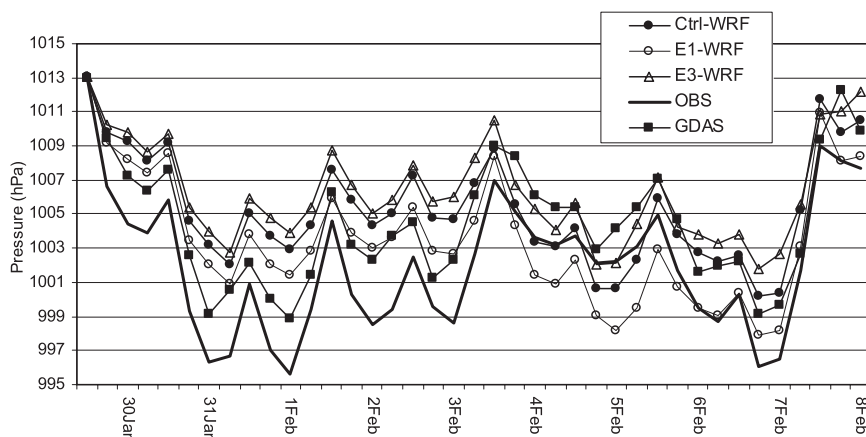


FIG. 2. Sea level pressure temporal evolution at La Rioja: the observation (solid line), GDAS analysis (filled squares), CTRL run (filled circles), E1 run (open circles), and E3 run (open triangles).

interest to this study. Figure 2 shows sea level pressure evolution at La Rioja (28°S, 66°W), a station located at the center of the NAL. This parameter is usually taken as a reference of NAL intensity (Seluchi et al. 2003). Surface pressure variability during the chosen NAL event is well reproduced by the CTRL run, compared with GDAS analysis and observed data. However, a tendency of the WRF model to underestimate the amplitude of the diurnal cycle is detected. Regardless of which model configuration is adopted (i.e., alternative land surface models, PBL parameterizations, and cumulus schemes), the WRF model exhibits this systematic bias over the region of interest (Ruiz et al. 2010). Figure 2 depicts two pressure fall cycles: one from 29 January to 1 February and the other from 3 to 7 February. In general, the CTRL run tends to underestimate the depth of the low pressure system. This can be more clearly appreciated with the aid of Fig. 3, which combines sea level pressure, 950-hPa winds, and 500–950-hPa thickness fields at three different stages of the system evolution: maximum depth during the first cycle (0000 UTC 1 February), initial phase of the second cycle (0000 UTC 3 February), and complete dissipation (1200 UTC 7 February). There is good agreement between model and GDAS fields; the NAL is correctly located (see the closed isobar with its center around 30°S, 66.5°W) though underestimated, and the low-level circulation is very well reproduced. The typical patterns associated with the weak SACZ phase, which include the NAL, the northerly wind enhancement in the central part of the continent, and the Atlantic anticyclone located west of its mean position, are also well represented.

Thickness fields are useful to identify the thermal character of the system (Seluchi et al. 2003) and also to recognize the area with stronger gradient associated with the location of a quasi-stationary front. Both are reasonably well captured by the simulation. The northward progression of the front by 7 February (Fig. 3, bottom panel) is accompanied by a retreat of the low pressure system from northwestern Argentina toward the area where it is maintained as the Chaco low. This modification characterizes the end of a NAL event [see Seluchi et al. (2003) for a discussion of the differences between one system and the other].

The accumulated precipitation associated with the event is shown in Fig. 4, which includes observations from available rain gauge network and model simulation. In general, there is good agreement, particularly regarding the area affected by heavy rain. Day-by-day inspection of simulated precipitation also denotes good agreement between observations and simulations (not shown). The CTRL run tends to produce light precipitation between 3 and 4 February, over the area around 27°S, 60°W, where it was not observed. Over the SACZ region,

the WRF model tends to overestimate precipitation. This is another manifestation of WRF systematic errors over the region of interest (Ruiz et al. 2010).

In general, we consider that the event is well represented by the CTRL run and is useful to the extent we need to support the experimental design and the conclusions we may derive from the sensitivity studies.

3. Impact of soil wetness changes on precipitation

Our first objective is to show how variations in soil wetness initial condition modify accumulated precipitation. Figure 5 shows the differences between each experiment and the CTRL run. Both E1 and E3 lead to the expected results: decreased soil wetness produces less precipitation and vice versa. Differences take place over the areas where precipitation was simulated, with major changes over central and eastern Argentina, Uruguay, southern Brazil, a band north of 15°S, and along the frontal area. In terms of relative importance (changes normalized by total simulated precipitation in the CTRL run, not shown) it can be noticed that larger impacts occur south of 20°S, regardless of whether soil wetness has been decreased or increased with respect to the CTRL run. Our difference fields for E1 and E3 look rather similar to Collini et al.'s (2008) results (see their Fig. 5), reinforcing our idea that this particular case is highly representative of an important component of the summertime variability.

The response to the localized sensitivity experiments is distinct from the regional ones, and one of the most interesting results is that the anomalies (Fig. 5) affect similar locations irrespective of the areas where soil wetness is modified. In E2 the response is consistent with a shift in the precipitation field, while in E4 there is a localized increase in rain centered over Uruguay, presumably associated with enhanced evaporation, combined with a shift in precipitation. Neither E2 nor E4 generates impacts over the SACZ precipitation region. In section 4, changes related with low-level circulation, which could account for the impact in precipitation particularly near the frontal position, are discussed with more detail.

To identify the pathways for land–atmosphere interactions it is useful to analyze the day-by-day evolution of soil wetness, precipitation, and convective available potential energy (CAPE). The area-average evolution of these fields over the box indicated in Fig. 5 is shown in Fig. 6. This box is representative of the area where the sensitivity is relatively large in all experiments. It is of interest to point out that area-average wilting point and saturation values are 0.088 and 0.498 m³ m⁻³, respectively, thus denoting that the experiments modify soil wetness contents between reasonable values. Splitting of

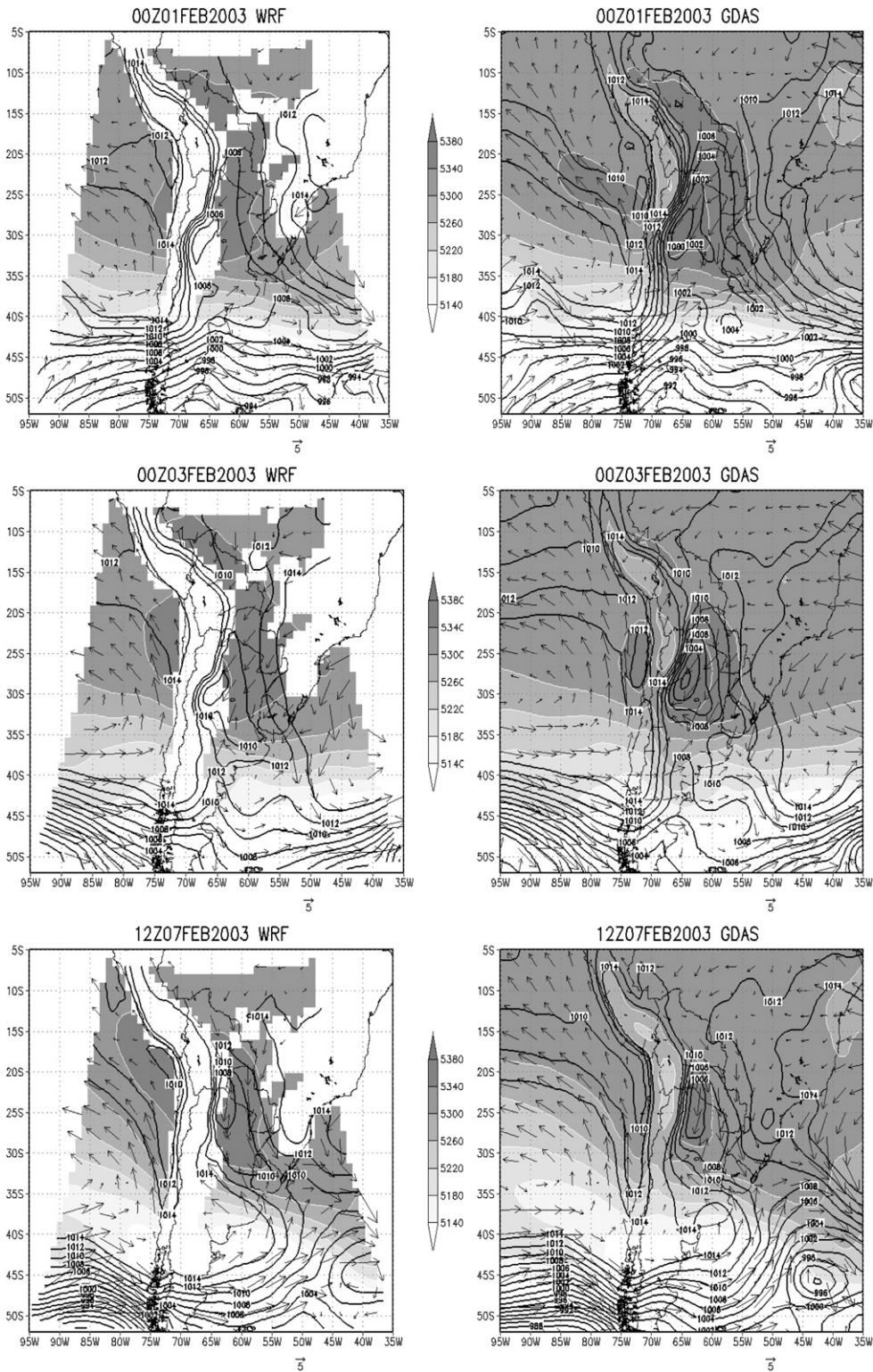


FIG. 3. Mean sea level pressure (contours, hPa), 500–950 thickness (shaded, m) and 950-hPa winds (vectors, m s^{-1}) at (top) 0000 UTC 1 Feb, (middle) 0000 UTC 3 Feb, and (bottom) 1200 UTC 7 Feb 2003. (left) CTRL simulation and (right) GDAS analysis.

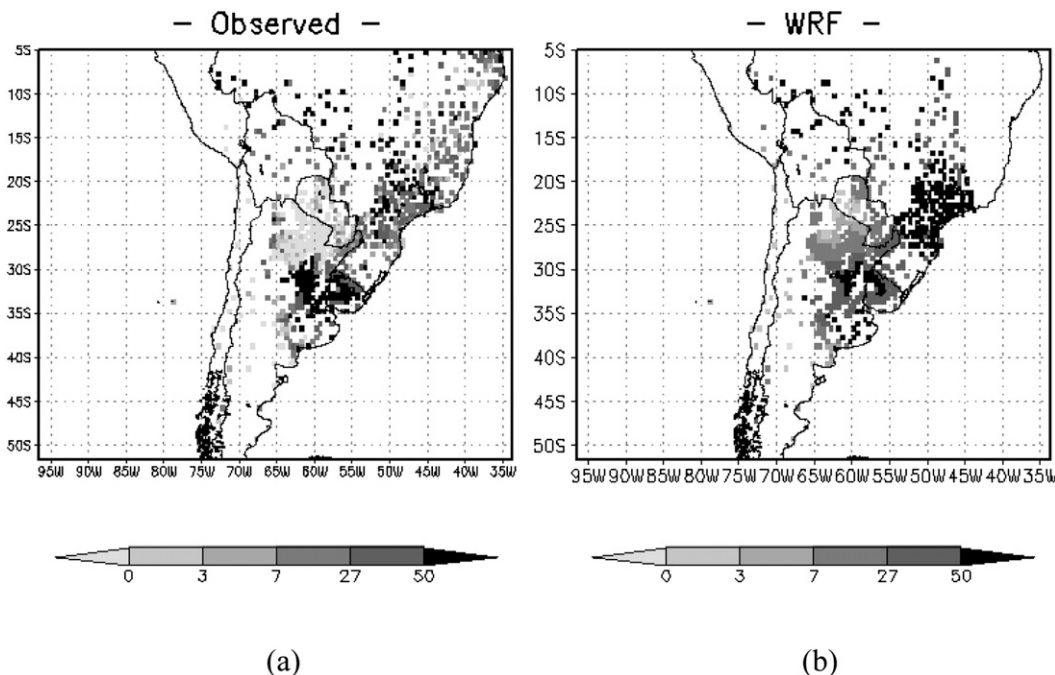


FIG. 4. (a) Rain gauge data and (b) CTRL run accumulated precipitation between 1200 UTC 29 Jan and 1200 UTC 7 Feb (mm). White boxes indicate grid areas where data are unavailable.

precipitation in its convective (i.e., that resulting from the cumulus scheme) and large-scale (i.e., that resolved explicitly) components has been done to follow an analysis similar to that of Pal and Eltahir (2001), who showed that the convective portion was much more sensitive to soil moisture changes than the large-scale one. As they state, convective rainfall in wet runs is facilitated because of two positive effects: lower cloud base and CAPE increases through low-level moistening. In contrast, dry runs, though warmer, result in very deep boundary layers (PBL) and lower CAPE. This response of the PBL to soil wetness has been confirmed in the present simulations, which exhibit the deepest PBL in E1, reaching almost twice the height of E3 on particular days (not shown).

Figure 6a shows the evolution of soil wetness for all the experiments. Soil moisture memory decreases with time, as expected: after 10 days of simulation, soil wetness differences become smaller, and all the experiments tend to the CTRL run. This is more evident for E2, E3, and E4, while in E1 the anomalous conditions appear to be more persistent. Given that soil wetness variations are hard to perceive, we plotted their anomalies (i.e., for each experiment we took the mean value and subtracted it from the actual value), which are shown in Fig. 6b. Besides a short adjustment period, there can be recognized a tendency of soil moisture to decrease up to 2 February and then a distinct phase characterized by continued increase.

The first question is how soil wetness changes drive precipitation changes and how precipitation modulates soil wetness. We address this issue with the aid of Figs. 6c,d. Changes in soil moisture affect the large scale and the convective portion of precipitation; however, given the small amount of large-scale precipitation involved (rain rates below 1 mm day^{-1}), the stronger impacts are associated with the convective portion of precipitation, as expected. If we compare E3 with E1 in Fig. 6c, it is clear that convective precipitation starts earlier when soil wetness is higher over the area. Besides the marginal precipitation in the first few days, the most important differences appear by 2 February (both in convective and large-scale portions). This helps to explain soil wetness behavior from the beginning of the model run: before rainfall occurrence (i.e., before 2 February) soil moisture evaporates, especially in experiments with increased soil wetness (E3 and E4 values decrease substantially, as seen in Fig. 6c). Just after this time, all the experiments except E1 show the start of heavier precipitation, and soil wetness recovers rapidly, with larger increases in close correspondence to larger rainfall rates. There is a sustained recuperation of soil wetness amounts from 3 February, which is more evident in the drier runs.

With regard to CAPE variability (Fig. 6e), it can be seen that experiments with higher CAPE have more convective rainfall (Fig. 6c). However, given similar CAPE

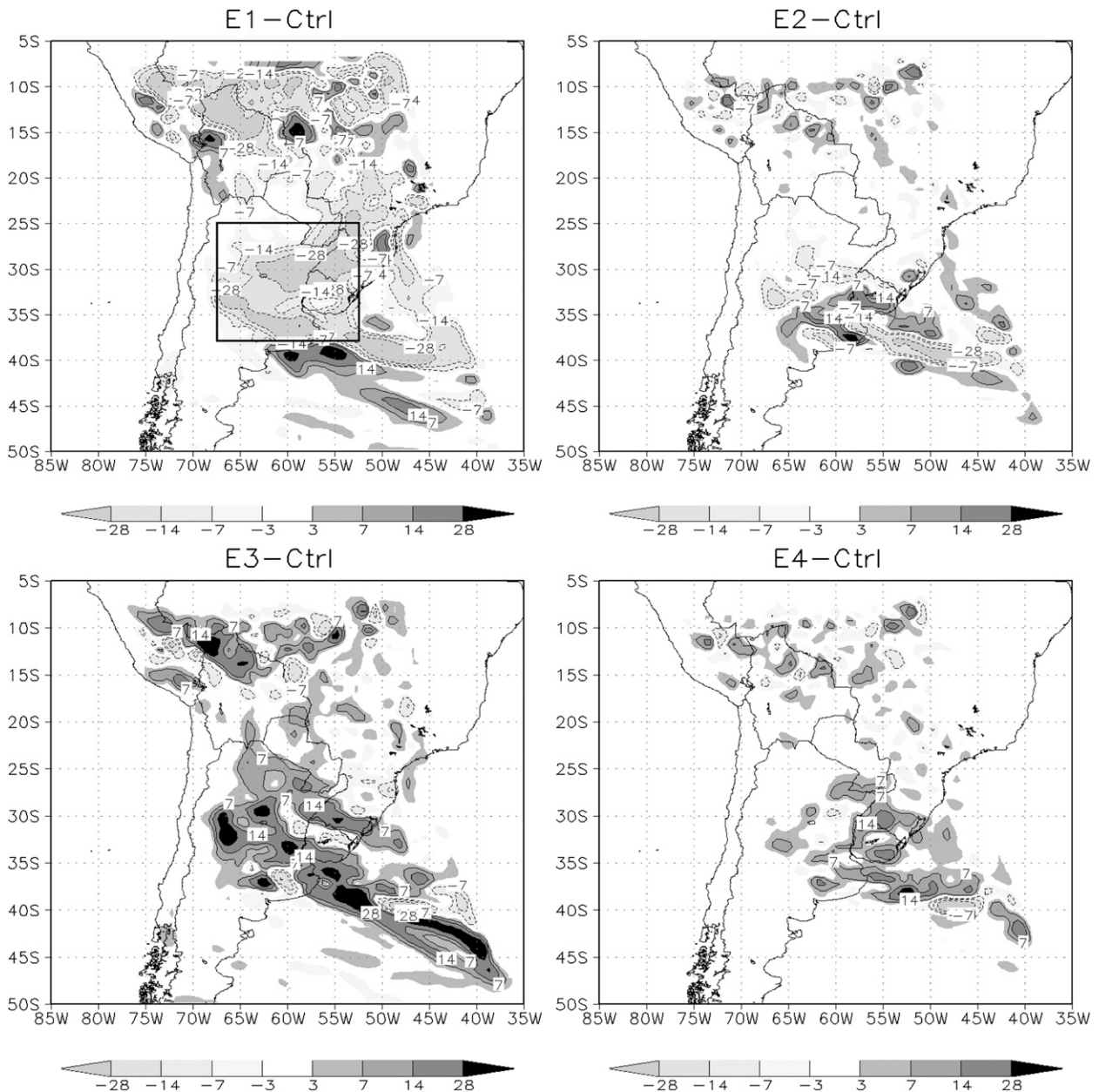
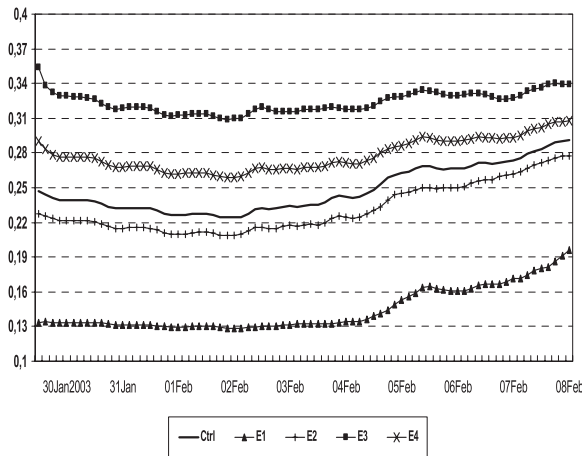


FIG. 5. Accumulated precipitation differences (mm) between each experiment and the control run. The box in the first panel indicates the area where averages have been performed.

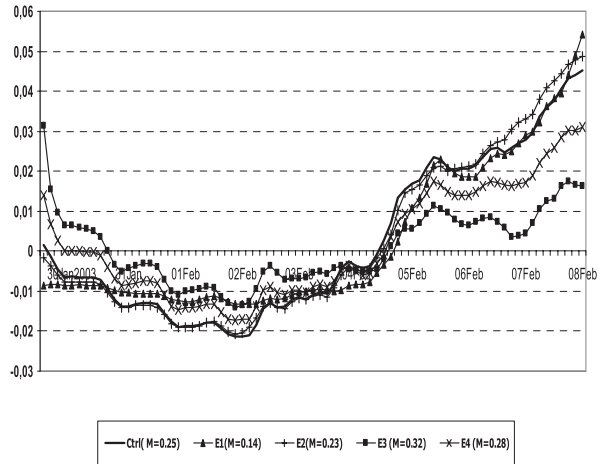
amounts from the beginning of the experiment until 3 February, significant precipitation does not start until 2 February. This indicates that changes in the circulation may have occurred between these dates. The diurnal cycle of CAPE—increasing between 1200 (approximately 0900 local time) and 0000 UTC, and decreasing afterward—is very similar for all the experiments except for E1. The particular diurnal cycle of CAPE in E1 is mostly explained by 2-m specific humidity variability that tends to maximize between 1200 and 1500 UTC (not shown).

The effect of CAPE diurnal cycle on precipitation diurnal cycle for all the experiments has also been analyzed. Unlike the behavior in the Great Plains, a clear delay between CAPE and precipitation maximum is not evident, at least through the analysis of area averages over the box of interest. This could be associated with the fact that the diurnal cycle of precipitation over this region is affected by different mechanisms and peaks alternatively in the night and/or daytime, as discussed by Nicolini and Saulo (2006). Still, when the synoptic

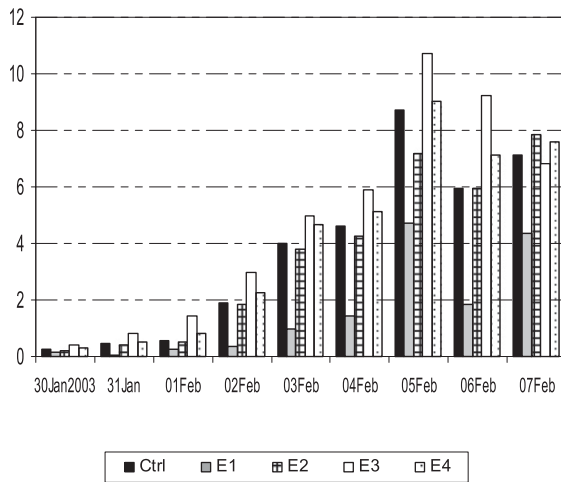
a) Soil wetness



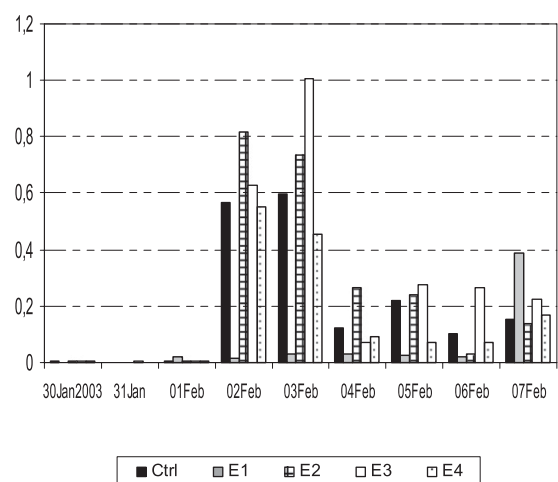
b) Soil wetness anomaly



c) Convective Precipitation



d) Large Scale Precipitation



e) CAPE

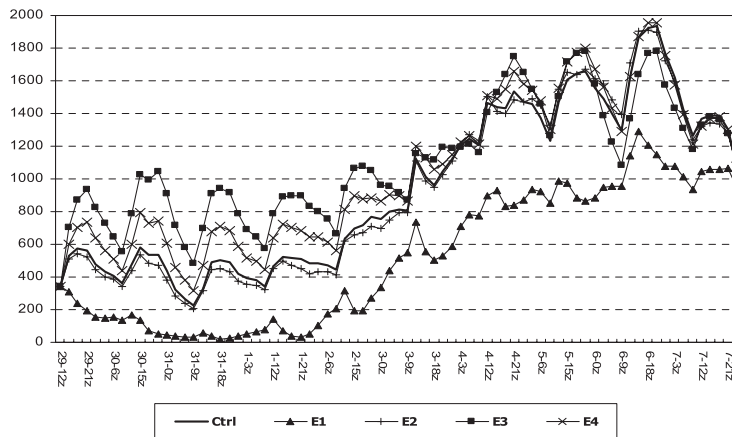
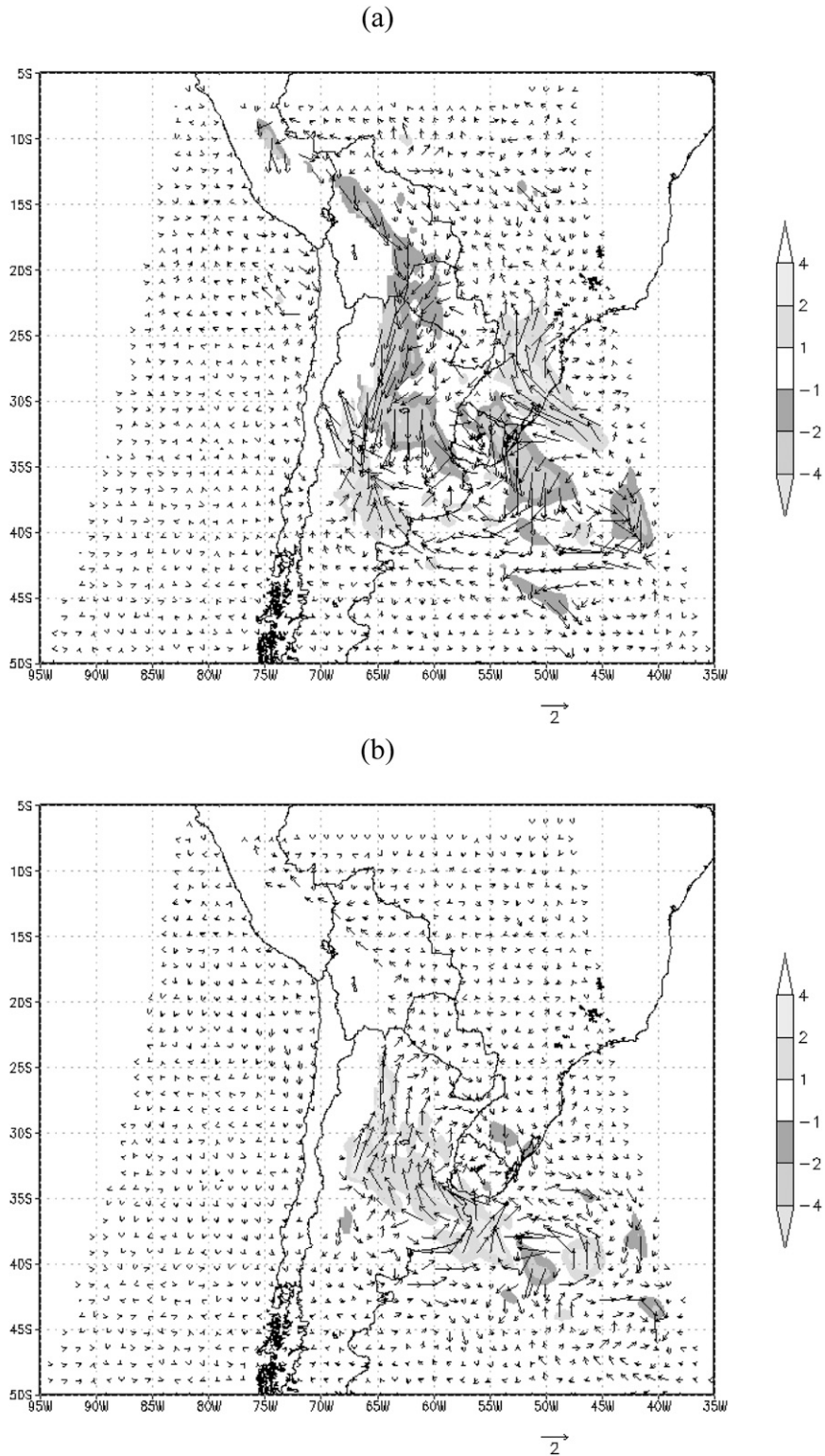


FIG. 6. (a) Soil wetness ($\text{m}^3 \text{m}^{-3}$), (b) soil wetness anomalies ($\text{m}^3 \text{m}^{-3}$), (c) daily accumulated convective precipitation (mm), (d) daily accumulated large-scale precipitation (mm), and (e) maximum CAPE (J kg^{-1}) area averaged over the box indicated in Fig. 5.



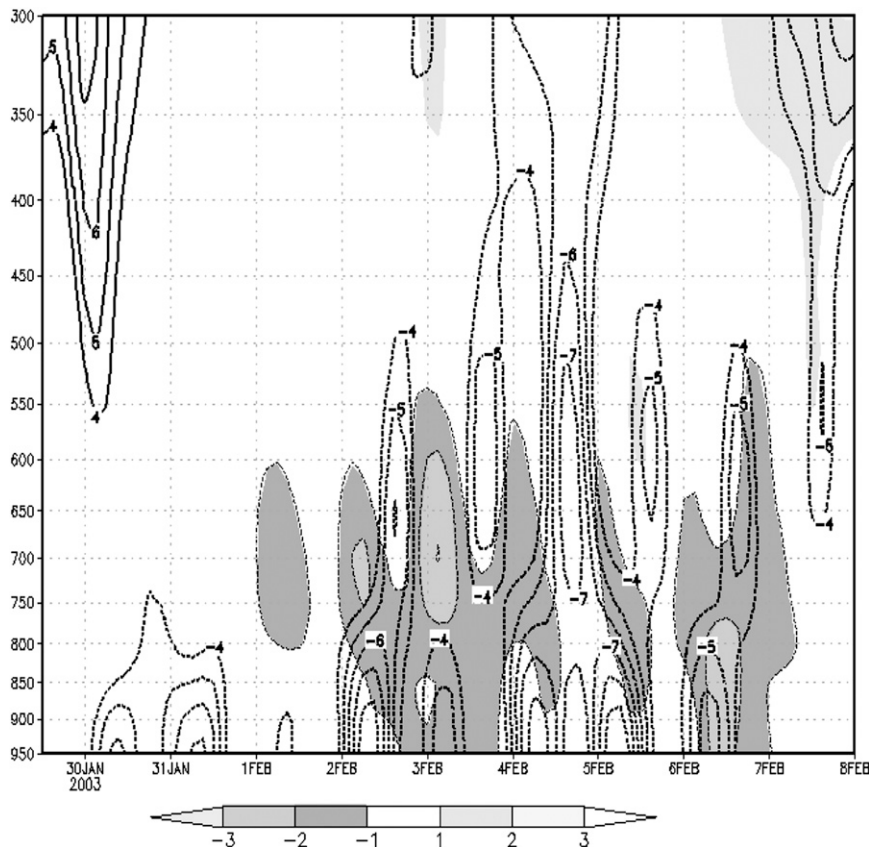


FIG. 8. Mean meridional wind speed (m s^{-1}) vertical cross section for the CTRL run (contours) and its anomaly ($\text{E1} - \text{CTRL}$, shaded), averaged in the box indicated in Fig. 5.

forcing is weak (up to 2 February), the CTRL run shows a 3–6-h delay between the CAPE and precipitation maxima. Section 4 provides extra information to analyze this diurnal cycle more in depth.

In terms of CAPE evolution, there is a strong similarity among CTRL, E2, E3, and E4 from 1200 UTC 3 February to the end of the simulation (i.e., from the second cycle). CAPE in E1 does not reach 400 J kg^{-1} until 3 February: this increase is accompanied by light but sustained convective precipitation, which explains the important recuperation of soil wetness between 4 February and the end of the model run. This is denoted by the increase of soil wetness rate during this last period. However, CAPE in E1 remains lower than that of the other experiments during the entire integration.

Up to this point we can recognize the following links: higher soil wetness produces larger CAPE and triggers earlier convective precipitation. This is a common feature among CTRL, E2, E3, and E4. Differences between these experiments—at least until 5 February—can be understood as a direct feedback between soil wetness amount and precipitation response: higher soil wetness leads to larger CAPE and associated precipitation.

Availability of surface moisture is maintained through this positive feedback between precipitation and surface conditions, leading to enhanced areal precipitation that characterizes all the experiments with normal or augmented moisture over SESA. This feedback is also evident in the dry run E1, but now reversed (i.e., drier soil and less precipitation). However, this coupling is partially overcome by an external forcing (in this case, of the synoptic scale) that increases CAPE—after 3 February—and leads to marginal precipitation, which increases the surface moisture, and changes E1 tendency, as a response to CAPE growth and the associated precipitation occurrence. After 7 days of simulation (by 6 February) CAPE is above 800 J kg^{-1} even in E1, with peak values related to moister runs that reach 1600 J kg^{-1} , while the amount of precipitation is considerably less for the drier runs.

4. Impact of soil wetness changes in the circulation

In the previous section we described the impact on precipitation and suggested local feedbacks that could aid in understanding the simulated behavior. We also need to

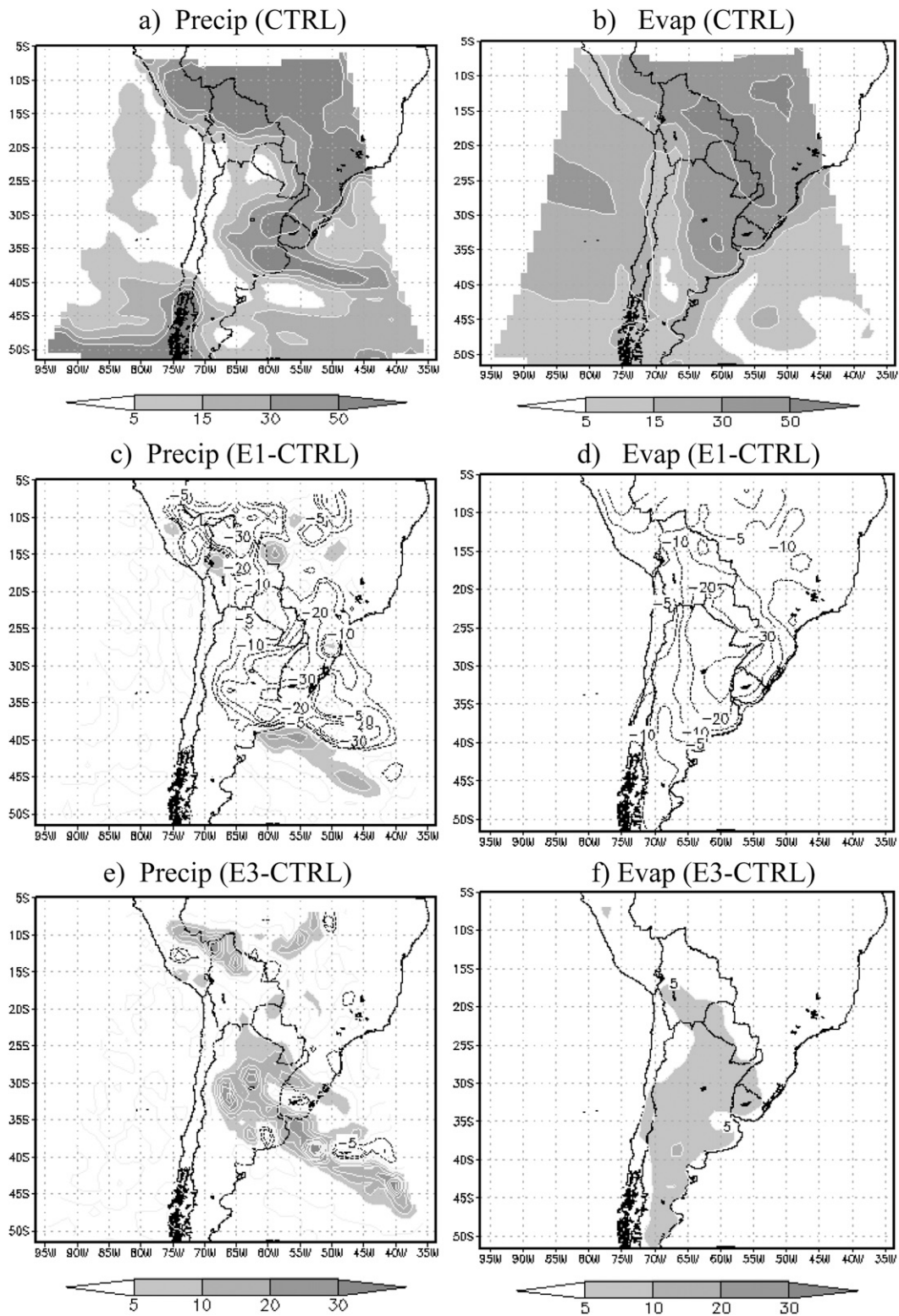


FIG. 9. Temporally integrated water vapor balance equation terms (mm) for the whole run. Positive values are shaded and negative ones are contoured. (a) CTRL precipitation, (b) CTRL evaporation, (c) E1 – CTRL precipitation, (d) E1 – CTRL evaporation, (e) E3 – CTRL precipitation, (f) E3 – CTRL evaporation, (g) CTRL water vapor flux convergence, (h) CTRL moisture storage change, (i) E1 – CTRL water vapor flux convergence, (j) E1 – CTRL moisture storage change, (k) E3 – CTRL water vapor flux convergence, and (l) E3 – CTRL moisture storage change.

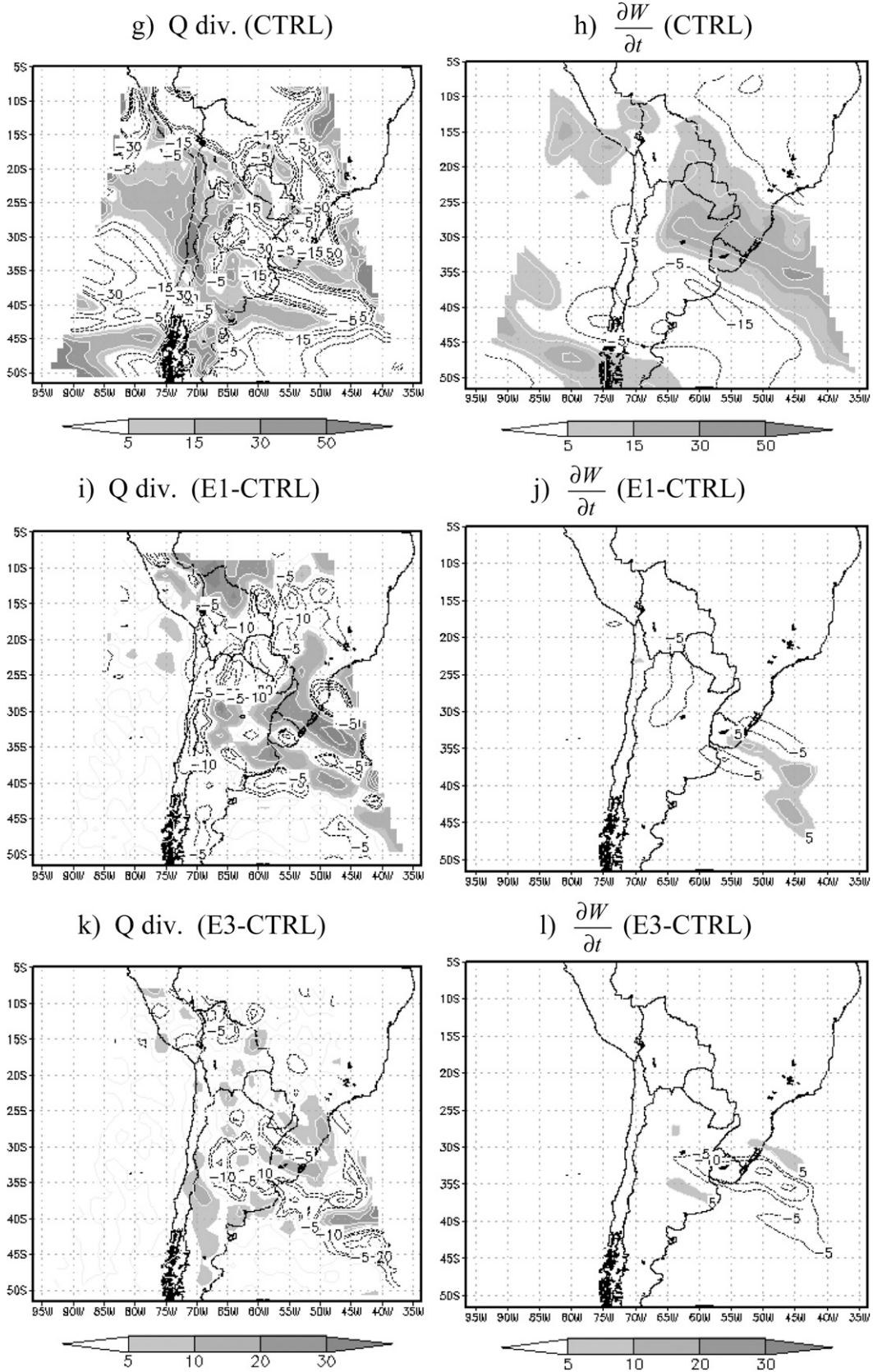


FIG. 9. (Continued)

understand if there is an advective contribution to rain that is being modified by soil wetness changes. To address this, we look at low-level 850-hPa winds, moisture convergence and the water budget integrated during the whole run. Unlike precipitation, it is not equally informative to simply average wind anomalies over the 10-day period. After analyzing the day-by-day evolution of the anomalies, we decided to synthesize them through their mean value at a particular UTC time. In this way we retain the major changes in circulation that occur at nighttime–early morning and are responsible for enhanced convergence at the exit region of the low-level jet (Saulo et al. 2004a; Nicolini and Saulo 2006; among others). Figure 7 shows the mean 850-hPa wind anomaly at 0600 UTC (approximately 0300 local time at 55°W) for E1 and E3. We have selected this UTC time because it depicts the highest anomaly values, while being representative of the patterns observed at 0300, 0900, and even 1200 UTC. The largest wind anomalies are evident in E1, followed by E3. Neither E2 nor E4 shows consistent wind anomalies on any day and/or UTC time (not shown). An interesting result is that circulation changes occur over an area that matches northerly wind core and frontal convergence regions, and does not fully coincide with the precipitation anomaly area (cf. Figs. 7a,b with Fig. 5). For the dry run, circulation anomalies over central portion of the domain are coherent with a geostrophic response to a deepened thermal low, as can be inferred looking at the evolution of sea level pressure at La Rioja (Fig. 2). The E1 simulates lower pressures throughout the whole run, at least compared with the other model runs. The opposite holds for E3, which tends to simulate the weakest NAL among the experiments, and is compatible with southerly anomalies close to the Andes, over central Argentina. Temporal evolution of wind changes—only for E1-CTRL—averaged over the same box used for previous analyses is shown in Fig. 8. This figure illustrates that, immersed in a sustained northerly wind current, that maximizes between 0300 and 0900 UTC (see contours), there are pulses of northerly anomalies that tend to reinforce and deepen the low-level jet. Similar figures have been constructed for all the experiments and, in all cases show much less impact—although not negligible—on a day-by-day basis.

To synthesize the impact of soil wetness changes in the circulation and the precipitation, we calculated the water vapor balance equation following Rasmusson (1967), expressed as

$$\frac{\partial W}{\partial t} + \nabla \cdot Q = E - P, \quad (1)$$

which states that changes in atmospheric moisture storage (W) in a column, are due to vertically integrated

water vapor flux divergence ($\nabla \cdot Q$), evapotranspiration from the surface (E), and precipitation (P). Vertical integration has been done between 1000 and 100 hPa. Usually, when integrated over a long period (more than a month) the first term in Eq. (1) is negligible, but, in our case, temporal variations of W cannot be disregarded. Figure 9 shows the integral for the whole simulation period of all the terms as represented by the CTRL run, and the corresponding differences with E1 and E3. Figures 9a,g show that, during this event, there is good correspondence between precipitation maxima and moisture flux convergence. Northeastward of the 30-mm E isopleth (Fig. 9b), evaporation also has a substantial contribution to the precipitation field. From the difference fields, it may be inferred that less precipitation in E1 over central and eastern Argentina, Uruguay, and southern Brazil is mostly explained by less evaporation, combined with decreased moisture convergence. The response in moisture convergence suggests that moisture reduction plays a dominant role in this field, compared with wind, that tends to increase convergence in a latitudinal band around 34°S (see Fig. 7a). Over the northern portion of the domain (part of Brazil, Peru, and Bolivia), evaporation is less related with precipitation decreases, which seem to be mostly explained by a reduction in moisture convergence. On the other hand, changes of precipitation in E3 closely follow those of increased moisture flux convergence differences, combined with a homogeneous increase in evaporation most apparent over Argentina. The other interesting signature in E3 comes from the W contribution that is negative, meaning that E3 has relatively higher rain efficiency than the control (less liquid water content is left in the column).

Over adjacent oceans there appear to be two distinct effects on E1: southward displacement of convergence seems to explain the resultant positive precipitation anomaly (south of Buenos Aires) and, increased W , combined with weakened moist convergence, aid in explaining the negative anomaly over the Atlantic (the one centered over 38°S, 47°W). A signature compatible with meridional displacement of convergence areas can also be noticed in E3. In general, the location of anomalous convergent areas is highly correlated with precipitation anomalies. Exceptions to this are E1 negative moisture flux divergence anomalies over northern Argentina, Paraguay, and southern Bolivia. This particular area exhibits a precipitation minimum in all the experiments.

The analysis of each of the balance equation terms for E2 and E4 shows that precipitation changes (see Fig. 5) are mostly explained by differences in the water vapor convergence terms, as seen in Fig. 10, where only this term is plotted.

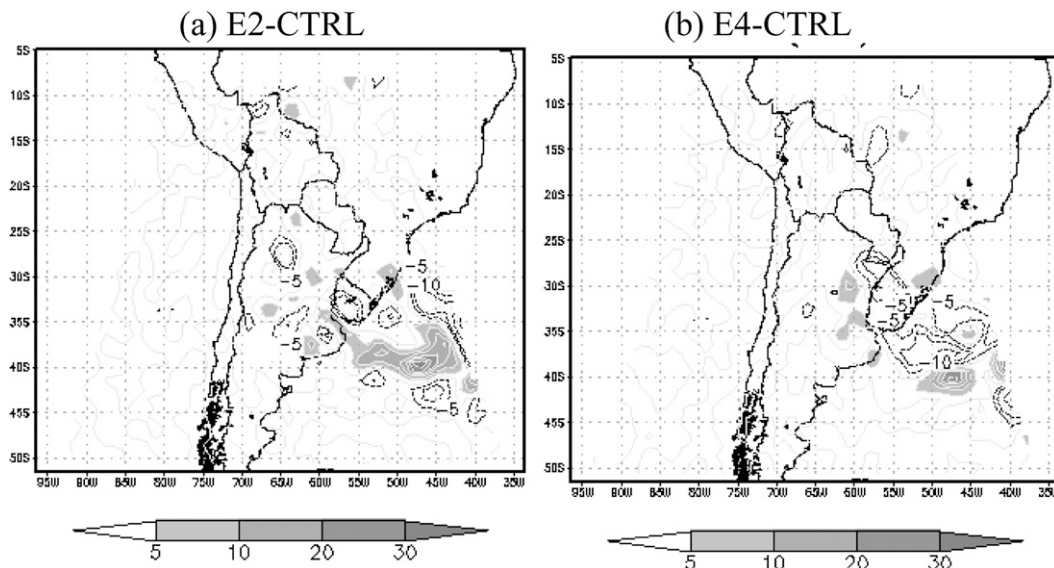


FIG. 10. Differences between (a) E2 and CTRL and (b) E4 and CTRL of the temporally integrated water vapor flux divergence term (mm) for the whole run. Negative values are contoured and positive ones are shaded.

Complementary information about the LLJ impact on the water budget can be incorporated with the aid of Fig. 11, where the diurnal cycle of the most important terms in the water balance equation (i.e., precipitation, evaporation, and water vapor flux convergence) have been averaged over the same box used in section 3. Looking at the CTRL run, it is evident that moisture convergence undergoes a change of regime by 2 February, from prevailing divergent conditions to the opposite situation. Superimposed with this trend, a nocturnal maximum in moisture flux convergence associated with the LLJ, can be recognized. In turn, accumulated precipitation generally maximizes around 2100 UTC, meaning that rain occurs mostly between 1800 and 2100 UTC (i.e., 0300 and 0600 local time), soon after CAPE (see Fig. 6e) and evaporation maxima. Consequently, precipitation between 0000 and 0900 UTC (night and early morning), has to be more strongly related with the LLJ and the associated moisture convergence. Under drier conditions as in E1, the diurnal cycle in wind convergence can be clearly recognized, but the magnitude of moisture flux convergence is smaller. This response, combined with less evaporation and less instability (Fig. 6e) explains the observed behavior in precipitation. When comparing E3 with the CTRL run, the most important differences are related with larger evaporation and moisture flux convergence with similar diurnal variations (not shown).

5. Summary and conclusions

The present experiments show sensitivity to soil wetness changes as measured by precipitation variations. In

turn, soil wetness rapidly reacts to rainfall, in such a way that after 10 days of simulation, the anomalous initial conditions tend to weaken. This response is not uniform over the model domain, and is more evident over SESA. The pathways relating soil–atmosphere interactions can be more easily tracked with the aid of E1 and E3: less (more) soil wetness reduces (enhances) CAPE so that precipitation—particularly its convective portion—is decreased (increased). This positive feedback is maintained during the first 5 days of simulation (i.e., until 3 February approximately) and corresponds to the first cycle of NAL pressure fall and the transition stage between the two cycles. The second phase is characterized by a stronger synoptic forcing, as suggested by the cleaner pressure cycle denoted in the evolution of sea level pressure at La Rioja, which also includes NAL decay by 1200 UTC 7 February (see the postfrontal anticyclone reaching central Argentina at this time in Fig. 3). This circulation is strong enough to initiate precipitation in E1, even under less favorable CAPE preconditioning, and to recover soil moisture deficits by the end of the simulation. Day-by-day inspection of the precipitation evolution (not shown) corroborates this analysis, and provides further details: the main difference between E1 and E3 is that in E3 there is strong prefrontal activity over Buenos Aires and central Argentina on 2 February not simulated by E1. This delay in convective triggering is crucial to understand soil influences at these time scales.

The analysis of the diurnal cycle provides additional insight into some mechanisms affecting precipitation: less soil moisture also affects the amount of water vapor

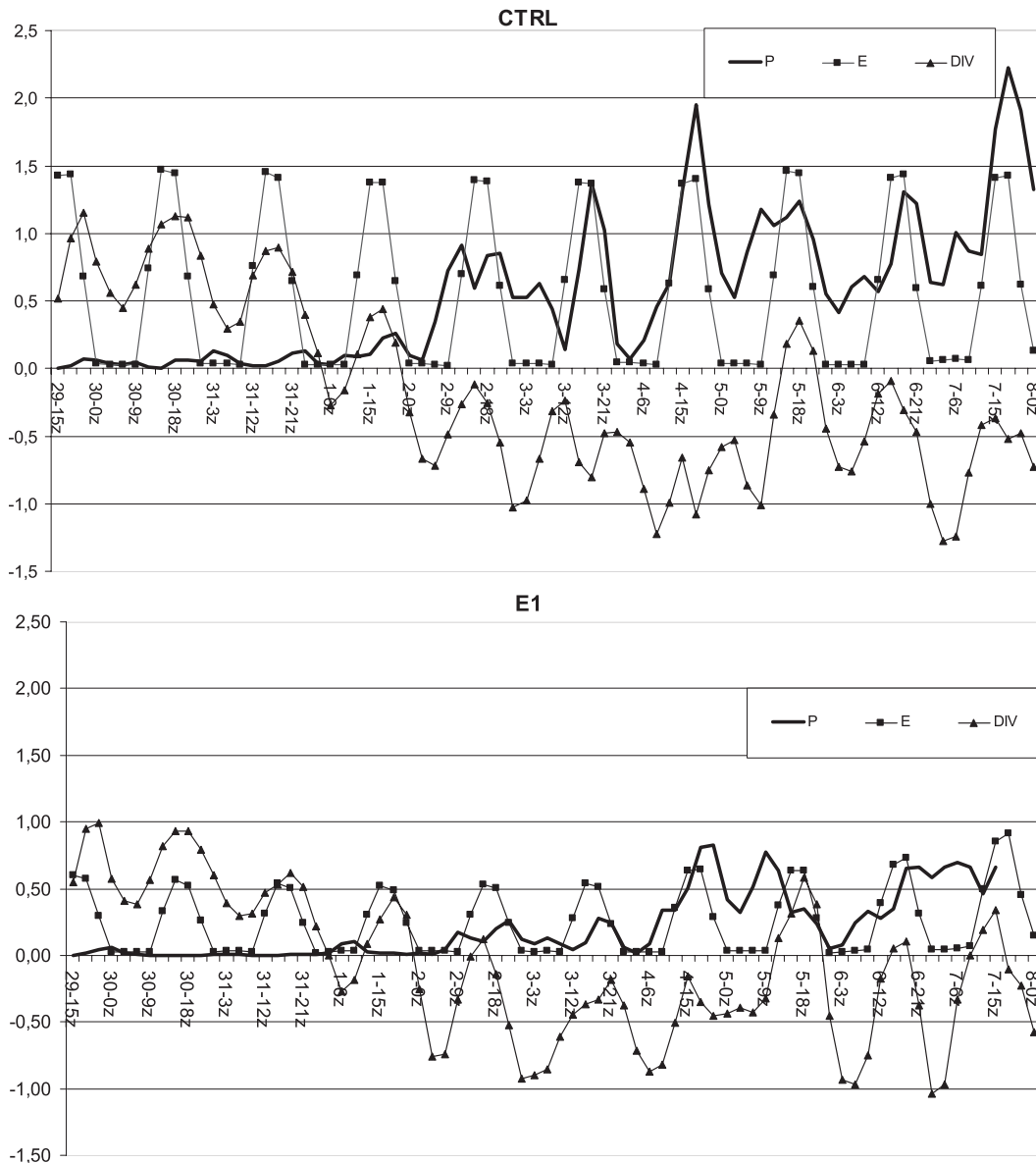


FIG. 11. Temporal evolution of precipitation, evaporation and water vapor flux convergence, area averaged over the box indicated in Fig. 5 (mm h^{-1}) for (top) the CTRL and (bottom) the E1 runs.

flux convergence and, consequently, the portion of precipitation that occurs during night and early morning hours. Still this feedback seems to be less important than that directly related with less moisture availability.

Looking at the circulation changes at regional scales, it is clear that low-level wind is more reactive to a reduction in soil wetness than to an increase of this parameter, and the response is as expected: an enhanced northerly wind, which results from a deepened NAL under dry conditions. The stronger northerlies in E1 can also explain the southward shift of the frontal precipitation, evident at the maritime portion of the front.

The wind response in E3 is weaker, compatible with reduced northerlies over central Argentina (i.e., associated with weaker NAL) and at the frontal area that can be related with the northward location of the precipitation maximum associated with the front.

The combined effects of changes in the circulation and in local stratification induced by soil wetness modifications, through variations in evaporation and CAPE, can be synthesized as follows: there is a dynamical response in the dry run, essentially associated to a stronger LLJ, that involves decreased convergence in the northwestern portion of the domain and enhanced convergence at the exit

region of the LLJ, which is displaced toward the south. This dynamical response is not as robust as that induced by less (more) evaporation and drier (moister) low-level air masses that result from lower (higher) soil wetness. These modifications also alter the stratification, in agreement with what has been found by Pal and Eltahir (2001). As a consequence, the moisture flux convergence pattern in E1 (E3), though different from the CTRL run, maintains its main features, but modulated by less (more) moisture availability. As a result, precipitation is more coherently modified where CAPE and moisture flux convergence variations mutually reinforce.

It is interesting to contrast these results with others obtained under different frameworks and/or motivations. For example, areas with larger sensitivity in our study coincide with areas highlighted by Dirmeyer et al. (2009) as having soil moisture controlling evapotranspiration, plus a climate regime tending to maintain soil moisture anomalies, which in turn become larger through recycling (see their Fig. 6). Also, that study identifies these areas as having relatively short soil moisture memory, concluding that prediction may benefit from careful initialization of soil conditions at forecast ranges below 30 days. This is in agreement with our results, since we found important differences in precipitation arising from changes in the initial soil moisture condition, which, in turn, are reinforced during a limited time period, and then tend to reduce.

We obtained somewhat different results from Collini et al. (2008), particularly with respect to wind changes during dry events, which, in our case, are more evident and extend to the surface. Also, they did not analyze the wet runs, since the impact was less coherent over their area of interest. Nonetheless, their discussion of the mechanisms that may explain their results is in complete agreement with what we found in our case study.

With regard to the interpretation of E2 and E4, we consider that a deeper analysis than the one performed here is needed. As already mentioned, the impact detectable in the accumulated precipitation can be almost totally explained by water vapor flux convergence and the pattern of rain change is not radically different between them. This is probably due to the fact that the areas selected to modify the soil condition, and the modification introduced (lowering soil wetness in E2 and increasing it in E4) are such that the final impact is not substantially different. We speculate that this may be attributed to a natural response of the system: no matter how we modify the initial condition, we obtain similar perturbations. Still, this hypothesis needs more experimentation. What can be stated from this preliminary analysis is that, at synoptic time scales, soil wetness reduction over northwestern Argentina and soil wetness increase over

SESA perturb the associated precipitation in a similar way (both regarding the area and the type of modification), with a slight preference for the latter to increase it (according to the area averages presented in Fig. 6). This result leaves a warning on possible impacts of enhanced irrigation over SESA agricultural area.

The current South American study is done in the spirit of earlier short-to-medium-range simulations for North America (i.e., Trier et al. 2008; Gallus and Segal 1999; Zhong et al. 1996) and it therefore emphasizes one case with relatively large soil moisture changes. From this case study it can be inferred that soil moisture has a significant impact on precipitation, and this impact becomes evident when the areas where precipitation is occurring are clearly identified. This denotes the value added by analyzing individual cases. Most of the changes in precipitation are due to changes in the availability of moisture at low levels. Modifications in the circulation are less evident and need even a more careful analysis in order to be recognized. Soil memory over the area of study is weak (cf. other regions) but enough to alter precipitation in a persistent way. For this reason, it is considered that this study further supports the importance of precise initial soil conditions in achieving maximum predictability at short and medium ranges.

Acknowledgments. This study has been supported by the following projects: NA06AR4310048 from NOAA/OGP/CPPA, ANPCyT PICT 2004 25269, UBACyT X204, CONICET PIP 112-200801-00399, 490225/2008-0 (Prosul), and 305302/2006-0 from CNPq. The research leading to these results has received partial funding from the European Community's Seventh Framework Programme (FP7/2007-2013) under Grant Agreement 212492 (CLARIS LPB; a Europe-South America Network for Climate Change Assessment and Impact Studies in La Plata Basin).

REFERENCES

- Anderson, J. R., E. E. Hardy, J. T. Roach, and R. E. Witmer, 1976: A land use and land cover classification system for use with remote sensor data. U.S. Geological Survey Professional Paper 964, 41 pp.
- Chen, S.-H., and J. Dudhia, 2000: Annual report: WRF physics. Air Force Weather Agency, 38 pp.
- Collini, E. A., E. H. Berbery, and V. Barros, 2008: How does soil moisture influence the early stages of the South American monsoon? *J. Climate*, **21**, 195–213.
- Compagnucci, R. H., and M. A. Salles, 1997: Surface pressure patterns during the year over southern South America. *Int. J. Climatol.*, **17**, 635–653.
- Dirmeyer, P. A., C. A. Schlosser, and K. L. Brubaker, 2009: Precipitation, recycling, and land memory: An integrated analysis. *J. Hydrometeorol.*, **10**, 278–288.

- Dudhia, J., 1989: Numerical study of convection observed during the winter monsoon experiment using a mesoscale two-dimensional model. *J. Atmos. Sci.*, **46**, 3077–3107.
- Fast, J., and M. McCorcle, 1990: A two-dimensional numerical sensitivity study of the Great Plains low-level jet. *Mon. Wea. Rev.*, **118**, 151–163.
- Ferreira, L., 2008: Causas y variabilidad de la Depresión del Noroeste Argentino e Impactos sobre los Patrones Regionales de Circulación (Causes and variability of the Northwestern Argentina Low and its impact over the regional circulations patterns). Ph.D. dissertation, 177 pp. [Available from Departamento de Ciencias de la Atmosfera, Ciudad Universitaria, 1428, Buenos Aires, Argentina.]
- Ferrier, B. S., Y. Jin, Y. Lin, T. Black, E. Rogers, and G. DiMego, 2002: Implementation of a new grid-scale cloud and precipitation scheme in the NCEP Eta model. Preprints, *15th Conf. on Numerical Weather Prediction*, San Antonio, TX, Amer. Meteor. Soc., 280–283.
- Gallus, W. A., and M. Segal, 1999: Diabatic effects on late-winter cold front evolution: Conceptual and numerical model evaluations. *Mon. Wea. Rev.*, **127**, 1518–1537.
- Grimm, A., J. S. Pal, and F. Giorgi, 2007: Connection between spring conditions and peak summer monsoon rainfall in South America: Role of soil moisture, surface temperature, and topography in eastern Brazil. *J. Climate*, **20**, 5929–5945.
- Hong, S.-Y., and H.-L. Pan, 1996: Nonlocal boundary layer vertical diffusion in a medium-range forecast model. *Mon. Wea. Rev.*, **124**, 2322–2339.
- Kain, J. S., 2004: The Kain–Fritsch convective parameterization: An update. *J. Appl. Meteor.*, **43**, 170–181.
- Lichtenstein, E. R., 1980: La Depresión del Noroeste Argentino (The Northwestern Argentina Low). Ph.D. dissertation, 223 pp. [Available from Departamento de Ciencias de la Atmosfera, Ciudad Universitaria, 1428, Buenos Aires, Argentina.]
- Marengo, J., W. R. Soares, C. Saulo, and M. Nicolini, 2004: Climatology of the low-level jet east of the Andes as derived from the NCEP–NCAR reanalyses: Characteristics and temporal variability. *J. Climate*, **17**, 2261–2280.
- Mlawer, E. J., S. J. Taubman, P. D. Brown, M. J. Iacono, and S. A. Clough, 1997: Radiative transfer for inhomogeneous atmosphere: RRTM, a validated correlated-*k* model for the long-wave. *J. Geophys. Res.*, **102** (D14), 16 663–16 682.
- Nicolini, M., and A. C. Saulo, 2006: Modeled Chaco low-level jets and related precipitation patterns during the 1997–1998 warm season. *Meteor. Atmos. Phys.*, **94**, 129–143, doi:10.1007/s00703-006-0186-7.
- Nogués-Paegle, J., and K. C. Mo, 1997: Alternating wet and dry conditions over South America during summer. *Mon. Wea. Rev.*, **125**, 279–291.
- Paegle, J., K. C. Mo, and J. Nogués-Paegle, 1996: Dependence of simulated precipitation on surface evaporation during the 1993 U.S. floods. *Mon. Wea. Rev.*, **124**, 345–361.
- Pal, J. S., and E. A. B. Eltahir, 2001: Pathways relating soil moisture conditions to future summer rainfall within a model of the land–atmosphere system. *J. Climate*, **14**, 1227–1242.
- Rasmusson, E. M., 1967: Atmospheric water vapor transport and the water balance of North America: Part I. Characteristics of the water vapor flux field. *Mon. Wea. Rev.*, **95**, 403–426.
- Rodell, M., and Coauthors, 2004: The Global Land Data Assimilation System. *Bull. Amer. Meteor. Soc.*, **85**, 381–394.
- Ruiz, J., C. Saulo, and J. Nogués-Paegle, 2010: WRF model sensitivity to choice of parameterization over South America: Validation against surface variables. *Mon. Wea. Rev.*, in press.
- Salio, P., M. Nicolini, and A. C. Saulo, 2002: Chaco low-level jet events characterization during the austral summer season by ERA reanalysis. *J. Geophys. Res.*, **107**, 4816, doi:10.1029/2001JD001315.
- Saulo, A. C., M. E. Seluchi, and M. Nicolini, 2004a: A case study of a chaco low-level jet event. *Mon. Wea. Rev.*, **132**, 2669–2683.
- , L. Ferreira, J. Mejia, and M. Seluchi, 2004b: Description of the thermal low characteristic using SALLJEX special observations. *CLIVAR Exchanges*, No. 9, International CLIVAR Project Office, Southampton, United Kingdom, 9–10 and 17.
- Schwerdtfeger, W. C., 1950: La depresión térmica del Noroeste Argentino. *Anales de la Sociedad científica Argentina*, Tomo CL, Buenos Aires, Argentina, 15 pp.
- Seluchi, M., A. C. Saulo, M. Nicolini, and P. Satyamurty, 2003: The northwestern Argentinean low: A study of two typical events. *Mon. Wea. Rev.*, **131**, 2361–2378.
- Skamarock, W. C., J. B. Klemp, J. Dudhia, D. O. Gill, D. M. Barker, W. Wang, and J. G. Powers, 2005: A description of the Advanced Research WRF Version 2. NCAR Tech. Note 468+STR, 100 pp.
- Sörensson, A. C., G. Menéndez, P. Samuelsson, U. Willén, and U. Hansson, 2010: Soil–precipitation feedbacks during the South American Monsoon as simulated by a regional climate model. *Climatic Change*, **98**, 429–447, doi:10.1007/s10584-009-9740-x.
- Trier, S. B., F. Chen, K. W. Manning, M. A. LeMone, and C. A. Davis, 2008: Sensitivity of the PBL and precipitation in 12-day simulations of warm-season convection using different land surface models and soil wetness conditions. *Mon. Wea. Rev.*, **136**, 2321–2343.
- Vera, C., and Coauthors, 2006a: Toward a unified view of the American monsoon systems. *J. Climate*, **19**, 4977–5000.
- , and Coauthors, 2006b: The South American Low-Level Jet Experiment (SALLJEX). *Bull. Amer. Meteor. Soc.*, **87**, 63–77.
- Wu, Y., and S. Raman, 1997: Effect of land use pattern on the development of low-level jets. *J. Appl. Meteor.*, **36**, 573–590.
- Xue, Y., F. De Sales, W. P. Li, C. Mechoso, C. Nobre, and H. Juang, 2006: Role of land surface processes in South American monsoon development. *J. Climate*, **19**, 741–762.
- Zhong, S., J. D. Fast, and X. Bien, 1996: A case study of the Great Plains low-level jet using wind profiler network data and high-resolution mesoscale model. *Mon. Wea. Rev.*, **124**, 785–805.

Copyright of Monthly Weather Review is the property of American Meteorological Society and its content may not be copied or emailed to multiple sites or posted to a listserv without the copyright holder's express written permission. However, users may print, download, or email articles for individual use.